

ALTITUDE VARIATION OF VERTICAL EXTENSIVE AIR SHOWERS IN THE UPPER PART OF THE ATMOSPHERE

R. A. ANTONOV, Yu. A. SMORODIN, and Z. I. TULINOVA

P. N. Lebedev Physics Institute, Academy of Sciences, U.S.S.R.

Submitted to JETP editor June 21, 1963

J. Exptl. Theoret. Phys. (U.S.S.R.) 45, 1865-1874 (December, 1963)

Experiments carried out in the upper part of the atmosphere yield data on the fluxes and spectra of vertical extensive air showers and also data on the lateral distribution of the shower particles. The altitude dependence of showers with  $\sim 10^6$  particles, derived on the basis of these data, indicates a high degree of energy dissipation in the interactions of particles with energies  $\sim 10^{15}$  eV which initiate the showers.

As is well known<sup>[1]</sup>, in the lower third of the atmosphere the altitude variation of extensive air showers (EAS) with a given number of particles depends little on the characteristics of the nuclear high-energy interactions that initiate the shower. In the upper part of the atmosphere, on the other hand, this dependence is strong. Therefore experimental data on the altitude variation in the upper layers of the atmosphere of showers with a given particle number is of great interest.

In view of the technical complexity of the experiments, the earlier studies<sup>[2-9]</sup> were devoted to the altitude variation of the counting rate of the coincidences of the discharges in the counters, which gave directly only the global altitude variation of the showers with given density. In an analysis of these data on showers having a density of approximately 50 particles/m<sup>2</sup>, Greisen<sup>[10]</sup> calculated the altitude variation of the showers with  $\geq 10^6$  particles. Several essential assumptions were made, in the calculations, the most important of which are the following:

- 1) The generalized Gross transformation, which yields the altitude variation of the vertical showers from data on the global altitude variation, is valid.
- 2) The particle-number spectra of the vertical showers obey a power law with exponent  $\kappa = 1.5$  at all altitudes.
- 3) The cascade parameter  $s$ , which characterizes the lateral distribution of the particles in the

shower, can be obtained from the shower absorption curve and differs little from unity for all altitudes.

The investigations described below enable us to check experimentally these assumptions and obtain the altitude variation of the showers with  $\sim 10^6$  particles on the basis of the experimental data.

The apparatus, the arrangement of which is shown in Fig. 1, has made it possible to determine the density of the particle flux in an air shower at three hodoscopic points and to pick out the showers whose axes were nearly vertical. To this end, the particle flux density in the shower was measured at the central hodoscopic point by two groups of counters. In one group the counter axes were vertical, and in the other they were horizontal. In each group there were 40 counters 30 mm in diameter and 300 mm long. To exclude the azimuthal asymmetry, the horizontal counters were divided into two groups, the axes of which were perpendicular to each other. The location of the vertical counters is shown in Fig. 1. At each of the peripheral points there were 20 counters of the same size.

The hodoscopic counters operated in the triggered pulse mode<sup>[11]</sup>. The triggering pulse was applied when four groups of counters, each of 860 cm<sup>2</sup> area, operated simultaneously. The triggering counters were placed under the hodoscopic counters of the central point.

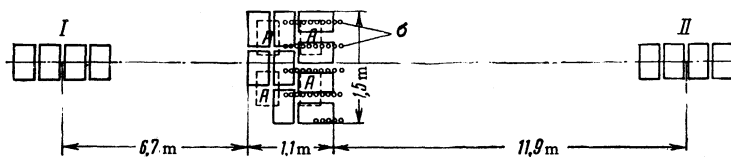


FIG. 1. Arrangement of apparatus (top view): A—boxes with triggering counters,  $\sigma$ —vertically oriented counter; I and II—peripheral counter groups.

To determine the zenith angle of incidence of the EAS, the method of area variation was used. The projection of the areas of the cylindrical counters on the plane perpendicular to the shower axes depends on the zenith angle. Therefore the probability that  $n$  horizontal and  $m$  vertical counters will operate in the shower depends on the zenith angle of incidence  $\theta_0$  of the shower:

$$W\left(\frac{m}{n}, \theta_0\right) = \int_0^\infty W_h\left(\frac{\rho}{n}\right) W_v\left(\frac{m}{\rho}\right) d\rho, \quad (1)$$

where

$$W_h\left(\frac{\rho}{n}\right) = [\rho^{-(\kappa'+1)} C_N^n (1 - e^{-\sigma_h \rho})^n e^{-\sigma_h \rho (N-n)}] \times \left[ \int_0^\infty \rho^{-(\kappa'+1)} C_N^n (1 - e^{-\sigma_h \rho})^n e^{-\rho \sigma_h (N-n)} d\rho \right]^{-1}, \quad (2)$$

$$W_v\left(\frac{m}{\rho}\right) = C_N^m (1 - e^{-\rho \sigma_v})^m e^{-\rho \sigma_v (N-m)}, \quad (3)$$

$N$  — total number of counters in the group,  $\sigma_h$  and  $\sigma_v$  — projections of the areas of the horizontal and vertical counters on the plane perpendicular to the shower axis.

In a shower whose axis has a zenith angle  $\theta_0$ , the electrons move as a result of scattering in directions  $\theta$  which differ from the axis direction. Theory<sup>[12,13]</sup> and experiment<sup>[14,15]</sup> indicate that the particle scattering can be approximated by a Gaussian distribution

$$\frac{dN}{d\delta} = \frac{1}{\sqrt{2\pi\alpha^2}} e^{-\delta^2/2\alpha^2}, \quad (4)$$

where  $\delta$  is the angle between the shower axis and the electron motion direction. According to experimental data on EAS at sea level<sup>[14,15]</sup>,  $\alpha$  lies in the interval 10–25°.

If  $\varphi$  is the angle that the plane passing through the vertical and the shower axis makes with the plane passing through the vertical and the electron trajectory, then

$$t = \cos \theta = \cos \delta \cos \theta_0 + \sin \delta \sin \theta_0 \cos \varphi. \quad (5)$$

The electron distribution in the shower of interest to us, with respect to the zenith angles  $\theta$ , or more accurately with respect to the quantities  $\cos \theta = t$ , can be expressed by the integral

$$\frac{dN}{dt} = \int_0^{2\pi} \frac{\partial^2 N}{\partial \varphi \partial t}(\varphi, t) d\varphi. \quad (6)$$

The integral (6) cannot be expressed in terms of elementary functions and was calculated by the Monte Carlo method for the mean-square scattering angles  $\alpha = 15^\circ$  and  $\alpha = 30^\circ$ .

These distributions make it possible to obtain

the probabilities  $W$  with allowance for the electron scattering in the shower:

$$W\left(\frac{m}{n}, \theta_0, \alpha\right) = \int_0^{\pi/2} W\left(\frac{m}{n}, \theta\right) \frac{dN}{dt}(t, \theta_0) \frac{dt}{d\theta} d\theta. \quad (7)$$

Figure 2 shows the values of  $W(m/20, \theta_0, \alpha)$  obtained from (7) for mean-square scattering angles 15 and 30°. We assume here  $\kappa' + 1 = 2.5$ .

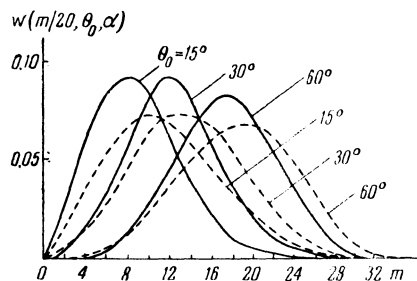


FIG. 2. Distribution of probabilities of the number of fired vertical counters  $m$  for fixed values of the number of operating horizontal counters ( $n = 20$ ), the shower axis angle of incidence  $\theta_0$ , and the values of the mean square electron scattering angle in the shower  $\alpha = 15^\circ$  (solid curves) and  $\alpha = 30^\circ$  (dashed curves).

The method of selecting the vertical showers was checked in a control experiment at sea level, where the angular distribution of the shower axes is known. In view of the fact that the width of the angular distribution of the shower axes at sea level is comparable with the mean-square scattering angle of the shower particles  $\alpha$ , an important role in the comparison of the calculations with experiment is played by the assumed value of  $\alpha$ . The experimental distribution of the showers with respect to the number of operating vertical counters agrees with the calculated distribution  $W(m)$  for a shower-axis angular distribution  $dN/d\theta_0 \sim \cos^l \theta_0$ , where  $l$  has a value 6–8 when  $\alpha$  is equal to 15–30°.

We used the above-described method of shower selection for a statistical separation of showers whose axes are inclined to the vertical by an angle  $\theta_0 \lesssim 30^\circ$ . The layers of atmospheric matter traversed by such showers differ from the layer of matter in the case of vertical incidence of the shower by less than 15%. It is obvious that to separate such EAS it is necessary to select events in which for a given  $n$  the number  $m$  does not exceed some  $m_0(n)$ . The counting rate of such showers is

$$N(n, m \leq m_0) = \int_0^{\pi/2} \frac{dN}{d\theta_0}(n, \theta_0) \sum_{m=0}^{m=m_0} W\left(\frac{m}{n}, \theta_0\right) \cdot 2\pi \sin \theta_0 d\theta_0. \quad (8)$$

The second factor under the integral sign decreases

with increasing  $\theta_0$ . We have chosen  $m_0$  such that not less than 75% of the events satisfying the criterion  $m \leq m_0(n)$  are showers for which the zenith angle is  $\theta_0 < 30^\circ$ .

The angular distribution of the shower axes  $dN/d\theta_0$  varies with altitude. We used in our calculations as a first approximation the angular distribution of showers calculated from the experimentally obtained global altitude variation of showers with given  $n$  with the aid of the Gross transformation [10,16].

Figure 3 shows the angular distributions of the shower axes  $dN/d\Omega(\theta_0)$ , obtained by the Gross transformation, and the integrands of (8) for  $n = 20$ ,  $m_0 = 9$ , and heights 6.4, 9, and 12 km. Using (8), we can easily calculate the values of the coefficients  $K$ , which make it possible to change from

the counting intensity of showers selected by the method described above to the differential counting intensity of the vertical EAS:

$$\frac{dN}{d\Omega}(\theta_0 = 0) = KN(m \leq m_0(n)). \tag{9}$$

Calculation shows that, as expected, the value of  $K$  depends little on the angular distribution of the shower axis and the degree of scattering of the particles in the showers. The uncertainty in the values of  $K$ , connected with the assumed approximation for  $dN(\theta_0)/d\Omega$ , does not exceed 10–15%.

Table I lists data characterizing the course of the experiment and the resultant experimental material.

Figure 4 shows the global spectra (summed over all angles) of the shower densities at different depths in the atmosphere. The spectra can be approximated by the power-law functions

$$\frac{dn}{dp} = A \left( \frac{p}{100 \text{ particles/m}^2} \right)^{-(\kappa'+1)}. \tag{10}$$

Figure 5 shows the density spectra for vertical showers. The same figure shows separately also data for showers whose axes pass far from the central hodoscopic point (see below). The spectra are approximated by power-law functions. The average value of  $\kappa' + 1$  for pressures 311 and 197 g/cm<sup>2</sup> is  $2.75 \pm 0.20$ . It must be noted that the last points on all the spectra fall on one side, and this may be due to the increase in the slope of the spectrum in the density region  $> 250$  particles/m<sup>2</sup>. If the dropped-out points are disregarded, then the average spectrum exponent decreases to  $2.6 \pm 0.2$ .

In determining the exponent of the particle-number spectrum of the showers, we start from the obtained density spectra of the vertical showers. If the form of the lateral distribution varies little with variation of the particle number in the shower, then  $\kappa = \kappa'$  in first approximation. In accordance with the results of Fig. 5, we have assumed that the spectral exponent for 197, 311, and 455 g/cm<sup>2</sup> is 1.7. Obviously, the value  $\kappa = 1.5$  used by Greisen [10], which agrees with the ex-

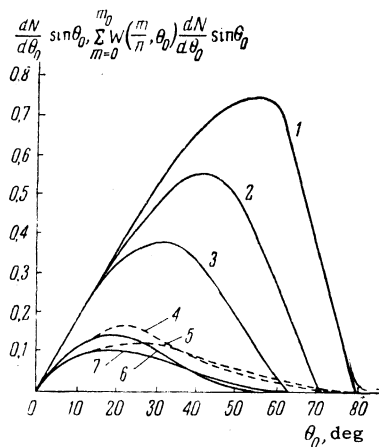


FIG. 3. Angular distributions of the axes of all the registered showers (curves 1–3) and the showers satisfying the selection rule  $m < m_0$  for values  $n = 20$  and  $m_0 = 9$  (curves 4–7). Curves 1, 4, and 5 correspond to a depth  $p = 197$  g/cm<sup>2</sup> (1—all showers, 4—selected showers for  $\alpha = 15^\circ$ , 5—selected showers for  $\alpha = 30^\circ$ ). Curves 2, 6, and 7 correspond to  $p = 311$  g/cm<sup>2</sup> (2—all showers, 6—selected showers for  $\alpha = 15^\circ$ , 7—selected showers for  $\alpha = 30^\circ$ ). Curve 3—all showers for  $p = 455$  g/cm<sup>2</sup>. The ordinates are  $(dN/d\theta_0)\sin\theta_0$  for curves 1–3 and  $\sum_{m=0}^{m_0} W(\frac{m}{n}, \theta_0) (dN/d\theta_0)\sin\theta_0$  for curves 4–7. All curves are so normalized that when divided by  $\sin\theta_0$  we obtain an ordinate 1.0 at  $\theta_0 = 0$ .

Table I

| Pressure $p$ , g/cm <sup>2</sup> | Measurement time, hours | Total number of showers | Number of showers with density at the central point $\rho_0 > 50$ particles/m <sup>2</sup> | Number of vertical showers in the density interval 110–280 particles/m <sup>2</sup> |
|----------------------------------|-------------------------|-------------------------|--|---|
| 1030                             | 250.2                   | 2 960                   | 772  | 189   |
| 455                              | 10.6                    | 7 444                   | 1 605  | 98  |
| 311                              | 34.0                    | 28 303                  | 6 731  | 411   |
| 197                              | 29.1                    | 20 573                  | 4 866  | 217   |
| 597                              | 0.40                    | 157                     | 39   |   |
| 392                              | 1.62                    | 1 432                   | 309  |   |

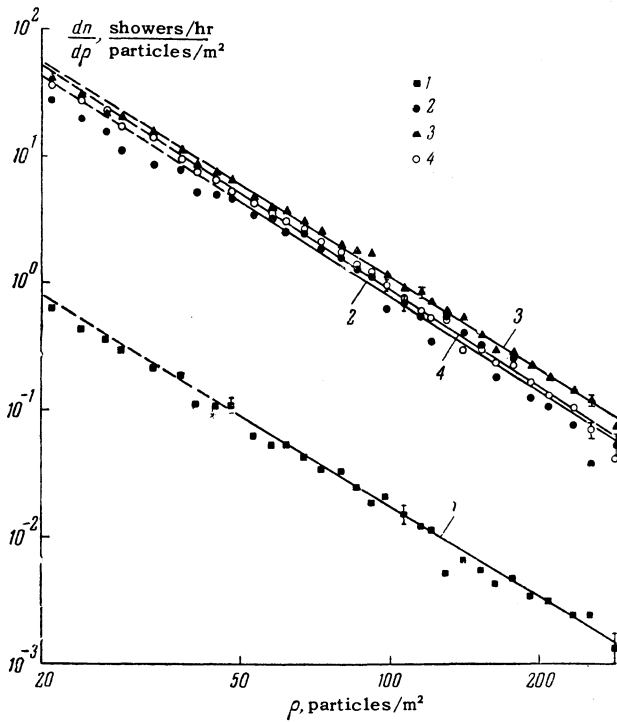


FIG. 4. Global spectra of shower densities for different depths of the atmosphere: 1— $p = 1030 \text{ g/cm}^2$ ,  $\kappa' + 1 = 2.4 \pm 0.2$ ,  $A = (1.7 \pm 0.15) \times 10^{-2}$ ; 2— $p = 455 \text{ g/cm}^2$ ,  $\kappa' + 1 = 2.5 \pm 0.15$ ,  $A = (8.3 \pm 0.6) \times 10^{-1}$ ; 3— $p = 311 \text{ g/cm}^2$ ,  $\kappa + 1 = 2.4 \pm 0.06$ ,  $A = 1.16 \pm 0.04$ ; 4— $p = 197 \text{ g/cm}^2$ ,  $\kappa' + 1 = 2.5 \pm 0.07$ ,  $A = (9.1 \pm 0.4) \times 10^{-1}$  (the statistical errors are not indicated for all the points). In the calculation of  $\kappa'$  and  $A$  by the method of least squares, the points corresponding to the dashed sections were not taken into account, since the corrections connected with the efficiency of the triggering system of counters plays a noticeable role for these points.

ponent of the global density spectra which we obtained, must be regarded as an underestimate.

If the development of the shower is determined only by the thickness of the layer of matter traversed by the shower in the atmosphere, then the intensity of the vertical flux of showers  $B(p)$  is connected with the global intensity  $C(p)$  by the Gross transformation<sup>[10,16]</sup>

$$B(p) = \frac{C(p)}{2\pi} \left( a + 1 - p \frac{\partial \ln C}{\partial p} \right). \quad (11)$$

The quantity  $a$  takes into account the effects due to the dependence of the shower registration efficiency on the angle of incidence. If the counting rate of the showers with given density varies with variation of the angle of incidence of the shower as  $\cos^a \theta$ , then the value of  $a$  in Eq. (11) is equal to this exponent. The calculation of  $a$ , carried out in accordance with Greisen<sup>[10]</sup>, leads to a value  $a = 1.4$ . The uncertainty in the value of  $a$  is due essentially to the uncertainty in the particle-number spectrum exponent  $\kappa + 1$ . In accordance with

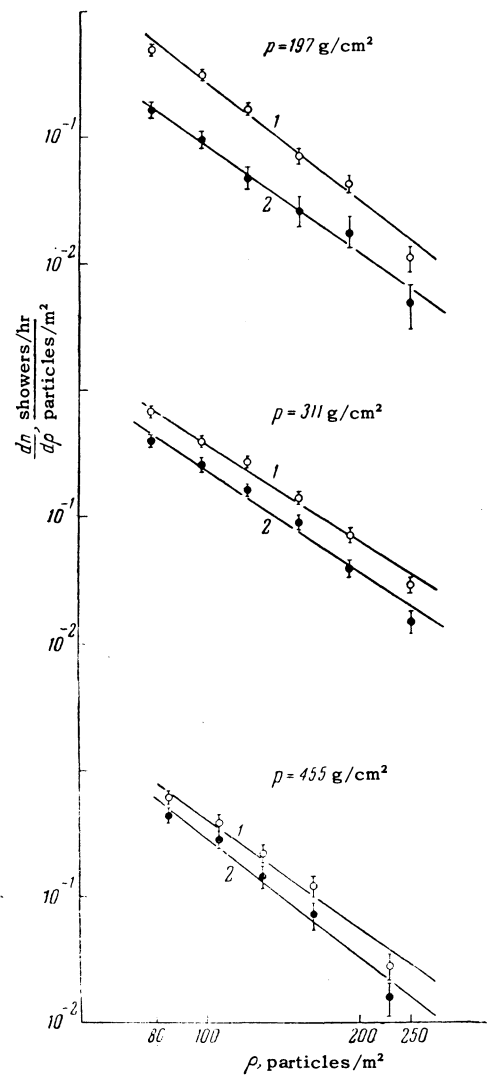


FIG. 5. Density spectra for vertical showers: 1—all vertical showers, 2—vertical showers satisfying the requirement  $\rho_7/\rho_0$  (or  $\rho_{12}/\rho_0$ )  $> 0.3$ . Case  $p = 197$ : curve 1— $\kappa' + 1 = 3.0 \pm 0.3$ ,  $A = (2.6 \pm 0.2) \times 10^{-1}$ ; curve 2— $\kappa' + 1 = 2.7 \pm 0.5$ ,  $A = (8.7 \pm 1.5) \times 10^{-2}$ . Case  $p = 311 \text{ g/cm}^2$ : curve 1— $\kappa' + 1 = 2.6 \pm 0.25$ ,  $A = (3.9 \pm 0.6) \times 10^{-1}$ , curve 2— $\kappa' + 1 = 2.7 \pm 0.3$ ,  $A = (2.4 \pm 0.4) \times 10^{-1}$ . Case  $p = 455 \text{ g/cm}^2$ : curve 1— $\kappa' + 1 = 3.0 \pm 0.5$ ,  $A = (4.3 \pm 0.9) \times 10^{-1}$ , curve 2— $\kappa' + 1 = 3.2 \pm 0.7$ ,  $A = (2.3 \pm 0.8) \times 10^{-1}$ .

the data of Figs. 4 and 5 we assume that  $\kappa + 1$  lies in the interval  $2.5 \leq \kappa + 1 \leq 2.7$  at the altitudes under consideration.

Figure 6 compares the results of the Gross calculation with the measured flux of vertical showers. The width of the shaded area corresponds to the statistical uncertainties in the quantities used in the calculation, including the uncertainty in  $\kappa$ . Some discrepancy between calculation and experiment, which can be seen in the figure, can be reduced by assuming that the spectrum exponent  $\kappa$  increases with altitude. Therefore the possibility of a perceptible influence of the decay

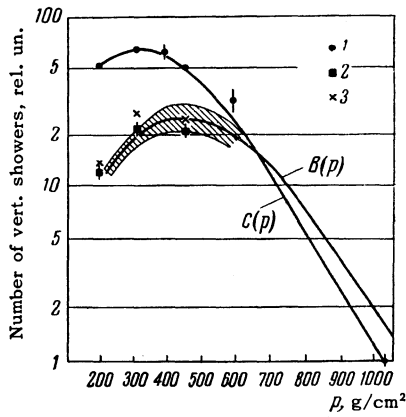


FIG. 6. Comparison of the Gross transformation with the data of measurements of the flux density of vertical showers: 1—all registered showers; 2—intensity of showers in vertical direction, referred to 1 steradian,  $\alpha = 15^\circ$ ; 3—the same as 2,  $\alpha = 30^\circ$ .

processes in the development of the extensive air shower, which we assumed in the preliminary reduction of the experimental material<sup>[17]</sup>, becomes less probable upon a detailed reduction.

To estimate the parameter  $s$ , which characterizes the lateral distribution of the particles in the shower, we have used data on the ratio of the density in the central point  $\rho_0$  to the peripheral densities  $\rho_7$  and  $\rho_{12}$ . If the form of the lateral distribution is given by the Nishimura-Kamata function  $f(r)$  and the particle-number spectrum of the shower is  $AN^{-\kappa}$ , then the number of showers with density  $\rho_0 > \rho$  at the center of the array is

$$n(>\rho) = \int_0^{r_0} A \left( \frac{\rho}{f(r)} \right)^{-\kappa} \cdot 2\pi r dr + \int_{r_0}^{\infty} A \left( \frac{\rho}{f(r)} \right)^{-\kappa} \cdot 2\pi r dr$$

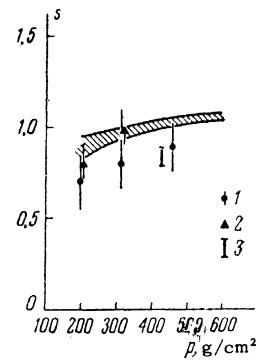
$$= A\rho^{-\kappa} \cdot 2\pi R_0^{-2(\kappa-1)} \left[ \int_0^{x_0} f(x)^\kappa x dx + \int_{x_0}^{\infty} f(x)^\kappa x dx \right], \quad (12)$$

where  $R_0$  is the Moliere unit in meters.

The integral with limits from 0 to  $r_0$  pertains to showers whose axes fall on the area of the central hodoscopic point. The second integral pertains to the passage of the axes outside the point. The first integral is approximately evaluated by numerical means. It was found that in calculating the first integral we can assume that  $r'$  is constant at 0.45–0.55 m. We note that this integral makes a small contribution to the total result.

The expression in the square brackets describes the lateral distribution of the shower axes. Using this distribution, we have calculated by the Monte Carlo method the distributions of the showers with respect to  $\rho_7/\rho_0$  and  $\rho_{12}/\rho_0$  for different values of  $s$ . The calculation of the values of  $P(\chi^2)$  for different  $s$  makes it possible to choose the best approximation for  $s$  (see Fig. 7).

FIG. 7. Variation of cascade parameter  $s$  with pressure: 1—data obtained by us (with allowance for an error  $\Delta\kappa = \pm 0.15$ ), 2—from [17], 3—from [9].



It is easy to see that when selecting the showers by density at the central point, the presence of fluctuations in the density leads to an underestimate of the ratios  $\rho_7/\rho_0$  and  $\rho_{12}/\rho_0$ , and by the same token to an underestimate of the value of  $s$ . In order to estimate the role of the fluctuations, we have also calculated the ratio  $\rho_7/\rho_{12}$  for showers of specified density  $\rho_0$ . The values of  $s$  describing this distribution were found to coincide with the values of  $s$  obtained from the distribution of the registered showers with respect to  $\rho_7/\rho_0$  and  $\rho_{12}/\rho_0$ . This coincidence shows that the fluctuations of the particle density in the shower are small.

Figure 7 shows a summary of the data on the variations of the cascade parameter  $s$ , describing the lateral distribution of the particles in the shower, with variation of the pressure. Along with the data obtained by the method described above, we also show the data (see [18]) which we obtained for the case when the axis position is determined by registering the electron-photon cascade with energy  $\gtrsim 10^{12}$  eV. We also show the point obtained from the data of Imai et al [9], who determined the density of the shower particles with the aid of four scintillation counters.

The shaded area gives the values of the age parameter  $s$ , which describes the absorption of the particles in the shower. They are calculated from the experimentally obtained (see below) altitude variation of the showers with  $\sim 10^6$  particles by the method described by Greisen<sup>[10]</sup>.

In order to reduce further the inaccuracy connected with the uncertainty of  $s$ , we have used the fact that the values of the functions  $f(x)$  depend little on  $x$  when  $0.02 \lesssim x \lesssim 0.2$ , that is, for showers whose axes pass sufficiently far away. We have selected such showers, for which one of the ratios  $\rho_7/\rho_0$  and  $\rho_{12}/\rho_0$  would be not less than 0.3. Then expression (12) changes into

$$n(>\rho) = A\rho^{-\kappa} R_0^{-2(\kappa-1)} \int_0^{2\pi} d\alpha \int_{x_{\text{lim}}}^{\infty} f^\kappa(x) x dx, \quad (13)$$

Table II

| Pressure $p$ ,<br>$g/cm^2$ | Exponent $\kappa$<br>integral<br>spectrum | Cascade<br>parameter<br>$s$ | Coeffi-<br>cient<br>$\theta$ | Intensity of verti-<br>cal showers<br>with density<br>100–300<br>particles/ $m^2$ | $N_{min} - N_{max}$             | Number of<br>showers<br>with $N >$<br>$10^6$ (B),<br>$m^{-2} sr^{-1}$ |
|----------------------------|---|-----------------------------|------------------------------|---|---------------------------------|---|
| 1030                       | 1.5                                       | 1.25                        | $3.3 \cdot 10^8$             | $0.90 \pm 0.07$   | $5 \cdot 10^5 - 7 \cdot 10^6$   | $2.7 \cdot 10^{-4}$   |
| 455                        | 1.7                                       | 0.9                         | $3.3 \cdot 10^8$             | $9.6 \pm 1.3$   | $2.5 \cdot 10^5 - 7 \cdot 10^6$ | $2.9 \cdot 10^{-3}$   |
| 311                        | 1.7                                       | 0.8                         | $2.5 \cdot 10^8$             | $10.0 \pm 0.7$  | $3 \cdot 10^5 - 6 \cdot 10^6$   | $4.0 \cdot 10^{-3}$   |
| 197                        | 1.7                                       | 0.7                         | $1.5 \cdot 10^9$             | $3.24 \pm 0.4$  | $3 \cdot 10^5 - 6 \cdot 10^6$   | $2.3 \cdot 10^{-3}$   |

where the limiting value  $x_{lim}$  is determined from the condition that  $\rho_7/\rho_0$  (or  $\rho_{12}/\rho_0$ ) exceeds 0.3.

If the particle number spectrum of the vertical showers is approximated by the expression

$$n(>N) = B \left(\frac{N}{10^6}\right)^{-\kappa} \frac{\text{Showers}}{m^2 hr-sr}, \quad (14)$$

then, by using (13), we can obtain the connection between the constant of the spectrum B and the number of registered vertical showers in the density interval  $100 \leq \rho \leq 300$  particles/ $m^2$ , satisfying the requirement that  $\rho_7/\rho_0$  (or  $\rho_{12}/\rho_0$ ) exceeds 0.3, namely

$$n(100 \text{ particles}/m^2 \leq \rho \leq 300 \text{ particles}/m^2) = B\Phi(\kappa, s, p). \quad (15)$$

The values of the coefficients  $\Phi$  and the analogous coefficients R for showers whose axes pass close to the central hodoscopic point ( $\rho_7/\rho_0 < 0.3$  and  $\rho_{12}/\rho_0 < 0.3$ ) were calculated for different values of  $\kappa$ ,  $s$ , and  $p$ . The calculation shows that  $\Phi$  depends little on  $s$ , whereas the dependence of R on  $s$  is much stronger. (When  $s$  or  $\kappa$  changes by an amount  $\sim 0.2$ , the value of  $\Phi$  changes by 30%, whereas the value of R changes under these same conditions by a factor of 4.)

Table II lists data characterizing the calculations of the shower particle-number spectra at different pressures. We also give the limiting particle numbers in the shower,  $N_{min}$  and  $N_{max}$ . For 70% of the showers used for the calculation, with densities 100–300 particles/ $m^2$ , the number of shower particles lies in this interval. The experimentally measured exponent for the density spectrum is a measure, in first approximation, of the particle-number spectrum exponent in the interval  $N_{min}-N_{max}$ .

The use for the calculations of the experimental data on the flux of the vertical showers with density from 100 to 300 particles/ $m^2$  is also necessitated by the fact that in this case the selection of the vertical showers and the determination of the ratios  $\rho_7/\rho_0$  and  $\rho_{12}/\rho_0$  are most accurate.

Figure 8 shows the altitude variation of showers

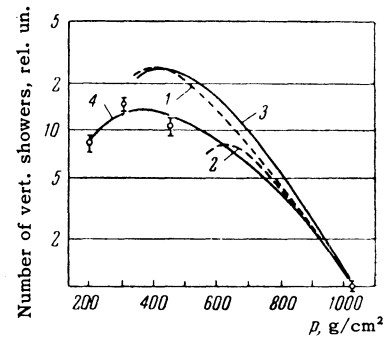


FIG. 8. Comparison of the experimental and calculated data on the altitude dependence of vertical showers with  $N > 10^6$  particles: 1—calculation,  $N = 10^6$ , interaction in accordance with the Landau model [1]; 2—calculation,  $N = 10^6$ , large fluctuations of energy transfer to one meson [1]; 3—calculation after Greisen,  $N > 10^6$ [10]; 4—curve drawn through our experimental data,  $N > 10^6$ .

>  $10^6$  particles. A comparison of the position of the maximum on the curve of the altitude variation with the calculations of [1] indicates that the particle energy is dissipated to a great degree in interactions which initiate the showers. The smearing of the maximum indicates the presence of appreciable fluctuations in the mechanism of energy transfer in the electron-photon component of the shower.

The authors take the opportunity to express deep gratitude to S. N. Vernov for help with the research.

<sup>1</sup>N. L. Grigorov and V. Ya. Shestoperov, JETP **34**, 1539 (1958), Soviet Phys. JETP **7**, 1061 (1958).

<sup>2</sup>H. L. Kraybill, Phys. Rev. **76**, 1092 (1949).

<sup>3</sup>A. L. Hodson, Proc. Phys. Soc. **A66**, 65 (1953).

<sup>4</sup>N. Hillberry, Phys. Rev. **60**, 1 (1941).

<sup>5</sup>A. T. Biehl and H. V. Neher, Phys. Rev. **83**, 1169 (1951).

<sup>6</sup>H. L. Kraybill, Phys. Rev. **93**, 1362 (1954).

<sup>7</sup>H. L. Kraybill, Phys. Rev. **93**, 1360 (1954).

<sup>8</sup>Imai, Kamata, Kawasaki, Murakami, and Takenchi, Scientific Papers of Inst. of Phys. and Chem. Research, Tokyo, **55**, 42 (1961).

<sup>9</sup>Imai, Kamata, Kawasaki, and Murakami, Proc. of the Intern. Conf. on Cosmic Rays and Earth Storm., Kyoto, **3**, (1961).

- <sup>10</sup> Cosmic Ray Physics (J. G. Wilson, ed.) North Holland, 1960, v. 3, ch I.
- <sup>11</sup> Antonov, Smorodin, and Tulinova, Trans. Intern. Conf. on Cosmic Rays, IUPAP, AN SSSR, 1959.
- <sup>12</sup> S. Z. Belen'kiĭ, Lavinnye protsessy v kosmicheskikh luchakh (Cascade Processes in Cosmic Rays), Gostekhizdat, 1960.
- <sup>13</sup> Dmitriev, Kulikov, Massal'skiĭ, and Khristiansen, JETP **36**, 992 (1959), Soviet Phys. JETP **9**, 702 (1959).
- <sup>14</sup> Z. S. Strugal'skiĭ, Dissertation, Moscow State University, 1957.
- <sup>15</sup> Guseva, Zatsepin, and Khristiansen, JETP **35**, 883 (1958), Soviet Phys. JETP **8**, 577 (1959).
- <sup>16</sup> D. V. Skobel'tsyn, Kosmicheskie luchi (Cosmic Rays), 1936.
- <sup>17</sup> Antonov, Smorodin, and Tulinova, Proc. of the Intern. Conf. on Cosmic Rays and the Earth Storm, Kyoto, **3**, (1961).
- <sup>18</sup> Antonov, Smorodin, and Tulinova, JETP **46**, 28 (1964), Soviet Phys. JETP **19**, in press.

Translated by J. G. Adashko